The dynamic range of the human metabolome revealed by challenges

Susanne Krug,*[,1] Gabi Kastenmüller,[‖,1] Ferdinand Stückler,[‖,1] Manuela J. Rist,[†,1] Thomas Skurk,*[,‡‡,1,2] Manuela Sailer,[†] Johannes Raffler,[‖,‖‖‖] Werner Römisch-Margl,[‖] Jerzy Adamski,[¶] Cornelia Prehn,[¶] Thomas Frank,[‡] Karl-Heinz Engel,[‡] Thomas Hofmann,[§] Burkhard Luy,[¶¶,##] Ralf Zimmermann,[#,***] Franco Moritz,[**] Philippe Schmitt-Kopplin,[**] Jan Krumsiek,[‖] Werner Kremer,[†††,‡‡‡,§§§] Fritz Huber,[†††] Uwe Oeh,[††] Fabian J. Theis,[‖,§§] Wilfried Szymczak,[††] Hans Hauner,*[,‡‡] Karsten Suhre,[‖,‖‖,‖‖‖] and Hannelore Daniel[†]

*Department of Nutritional Medicine, Research Center for Nutrition and Food Sciences, [†]Molecular Nutrition Unit, [‡]Department of General Food Technology, and [§]Department of Food Chemistry and Molecular Sensory Science, Technische Universität München, Freising-Weihenstephan, Germany; [‖]Institute of Bioinformatics and Systems Biology, [¶]Institute of Experimental Genetics, Genome Analysis Center, [#]Comprehensive Molecular Analytics Cooperation Group, Joint Mass Spectrometry Centre, [**]Analytical Biogeochemistry Research Unit, and [††]Medical Radiation Physics and Diagnostics Research Unit, Helmholtz Zentrum München, Neuherberg, Germany; [‡‡]Klinikum Rechts der Isar and [§§]Department of Mathematics, Technische Universität München, Munich, Germany; [‖‖]Faculty of Biology, Ludwig-Maximilians-Universität, Planegg-Martinsried, Germany; [¶¶]Institute of Organic Chemistry and [##]Institute for Biological Interfaces II, Karlsruhe Institute of Technology (KIT), Karlsruhe, Germany; [***]Department of Analytical Chemistry, University of Rostock, Rostock, Germany; [†††]LipoFIT Analytic GmbH, Regensburg, Germany; [‡‡‡]Institute of Biophysics and Physical Biochemistry and [§§§]Center for Magnetic Resonance in Chemistry and Biomedicine, University of Regensburg, Regensburg, Germany; and [‖‖‖]Department of Physiology and Biophysics, Weill Cornell Medical College in Qatar, Doha, Qatar

ABSTRACT   Metabolic challenge protocols, such as the oral glucose tolerance test, can uncover early alterations in metabolism preceding chronic diseases. Nevertheless, most metabolomics data accessible today reflect the fasting state. To analyze the dynamics of the human metabolome in response to environmental stimuli, we submitted 15 young healthy male volunteers to a highly controlled 4 d challenge protocol, including 36 h fasting, oral glucose and lipid tests, liquid test meals, physical exercise, and cold stress. Blood, urine, exhaled air, and breath condensate samples were analyzed on up to 56 time points by MS- and NMR-based methods, yielding 275 metabolic traits with a focus on lipids and amino acids. Here, we show that physiological challenges increased interindividual variation even in phenotypically similar volunteers, revealing metabotypes not observable in baseline metabolite profiles; volunteer-specific metabolite concentrations were consistently reflected in various biofluids; and readouts from a systematic model of β-oxidation (*e.g.*, acetylcarnitine/palmitylcarnitine ratio) showed significant and stronger associations with physiological parameters (*e.g.*, fat mass) than absolute metabolite concentrations, indicating that systematic models may aid in understanding individual challenge responses. Due to the multitude of analytical methods, challenges and sample types, our freely available metabolomics data set provides a unique reference for future metabolomics studies and for verification of systems biology models.—Krug, S., Kastenmüller, G., Stückler, F., Rist, M. J., Skurk, T., Sailer, M., Raffler, J., Römisch-Margl, W., Adamski, J., Prehn, C., Frank, T., Engel, K.-H., Hofmann, T., Luy, B., Zimmermann, R., Moritz, F., Schmitt-Kopplin, P., Krumsiek, J., Kremer, W., Huber, F., Oeh, U., Theis, F. J., Szymczak, W., Hauner, H., Suhre, K., Daniel, H. The dynamic range of the human metabolome revealed by challenges. *FASEB J.* 26, 2607–2619 (2012). www.fasebj.org

IN BIOFLUIDS OR TISSUES, metabolomics identifies and quantifies the final entities of the reaction chain along

---

[1] These authors contributed equally to this work.
[2] Correspondence: Else Kröner-Fresenius-Center for Nutritional Medicine, Technische Universität München, Gregor-Mendel-Str. 2, 85350 Freising, Germany. E-mail: skurk@tum.de

the paradigm of biology, from genes to transcripts to proteins to the metabolic intermediates. In contrast to the other profiling technologies, such as transcriptomics or proteomics, metabolomics data can be better interpreted on the basis of biochemical knowledge gained over almost a century. For diagnostic purposes, metabolic analysis of body fluids was first established for inborn errors of metabolism, based on the pioneering work of A. Garrod, "The Incidence of Alkaptonuria: A Study in Chemical Individuality," published in 1902 (1), and is now standard in newborn screenings (2). More recent developments propose metabolomics as a biomarker discovery tool for a variety of diseases, including Crohn's disease, Parkinson's disease, or cancer (3–5). While markers that associate with a manifest disease are often readily detected, it is far more difficult to determine the status of health and define the border between health and disease. Early alterations in metabolism, however, might be unmasked by challenging metabolic regulatory processes, testing the individual capacity and flexibility to cope with environmental stressors, such as physical activity or dietary components. However, most metabolomics studies to date are limited to the analysis of samples obtained in a fasted state, and only very few studies report time-resolved changes of the human metabolome in response to a challenge (6–8). Using a liquid chromatography–tandem mass spectrometry (LC-MS/MS) method with detection of 191 metabolites in plasma samples derived during an oral glucose tolerance test (OGTT) in healthy and prediabetic volunteers, Shaham et al. (6) identified metabolites with significant changes not previously described in the context of glucose homeostasis, such as bile acids or urea cycle intermediates. Rubio et al. (8) revealed numerous new fasting markers by analyzing metabolite profiles of plasma and urine sampled during extended fasting in human volunteers with multivariate statistics. Wopereis et al. (7) analyzed metabolome changes during an OGTT in overweight human volunteers during a 9-wk intervention with a mild acting anti-inflammatory drug and demonstrated that the OGTT increased the statistical power for detecting differences by treatment.

To extend the knowledge on the dynamics of the human metabolome in response to diverse challenges, we performed a study in which 15 healthy male volunteers underwent 6 different challenges over 4 d of study: a prolonged fasting period of 36 h (fasting), a standard liquid diet (SLD), an OGTT, an oral lipid tolerance test (OLTT), a physical activity test (PAT), and a cold pressure stress test (stress). Within this study, a variety of sample types [blood, urine, exhaled breath, and exhaled breath condensate (EBC)] were collected with high temporal resolution (on up to 56 time points) and analyzed with NMR and different mass spectrometric techniques, mainly focusing on lipids and amino acids. The present work aims to describe the challenges and metabolic analysis protocols and to present examples of our data according to the 3 directions of our human metabolome study: the analyt-ical depth (different methods), the breadth of the physiological challenges (different metabolic conditions) and the width of the sample coverage (different biofluids and high sampling frequency). In addition, we show an application of metabolome data for systems biology. To our knowledge, no other study has yet characterized the dynamics of human metabolome in a more detailed manner. This study, with >2100 individual samples, provides a valuable data set of the metabolome under various physiological conditions, measured on different analytical platforms and in different biofluids. The metabolomics data obtained within this study are freely and permanently available online [Human Metabolome Study (HuMet); http://metabolomics.helmholtz-muenchen.de/humet].

MATERIALS AND METHODS

Subjects

Volunteers were recruited into the human study center of the Else Kröner-Fresenius Center for Nutritional Medicine (Technische Universität München, Munich, Germany). After medical examination, 15 healthy, young and normal weight men were included into the study. They showed no metabolic abnormalities based on standard clinical chemistry, did not take any medication, and gave their written informed consent. The study protocol was approved by the ethical committee of the Technische Universität München (#2087/08) and corresponds with the Declaration of Helsinki.

Entrance examination

During a medical examination, standard clinical (blood lipids, blood pressure. etc.) and anthropometric parameters, such as body mass index (BMI), waist-to-hip ratio, etc., were determined. The resting metabolic rate (RMR) was measured by indirect calorimetry (Deltatrac metabolic monitor; Datex-Ohmeda, Helsinki, Finland). Body composition was assessed by dual energy X-ray absorptiometry using an Explorer bone densitometer (Hologic Inc., Bedford, MA, USA). Individual anaerobic threshold was assessed with an incremental bicycle ergometer test starting at 50 W at the Center for Prevention and Sports Medicine (Technische Universität München).

Study design

The study design, showing the sequence of challenges, is displayed in **Fig. 1**. Volunteers underwent 6 challenges within 2 test periods, each lasting 2 days and 2 nights. In the 24 h before each test period, subjects were asked not to consume alcohol or to undertake strenuous physical exercise. To minimize environmental influences on the metabolome, subjects stayed inside the study unit throughout both study periods under controlled food and fluid intake and physical activity. Volunteers were admitted to the study unit on the evening before each test period to consume a standardized balanced meal at 7 PM (503 kJ/100 g) with mineral water. Besides the challenge meals, subjects received a standardized breakfast at 8 AM (d 2), lunch at 12 PM (d 3), and dinner at 7 PM (d 3), which always consisted of a commercial fiber-free formula drink (Fresubin Energy Drink, chocolate flavor; Fresenius Kabi, Bad Homburg, Germany). The energy content of all defined meals was adjusted to 1/3 of the individual
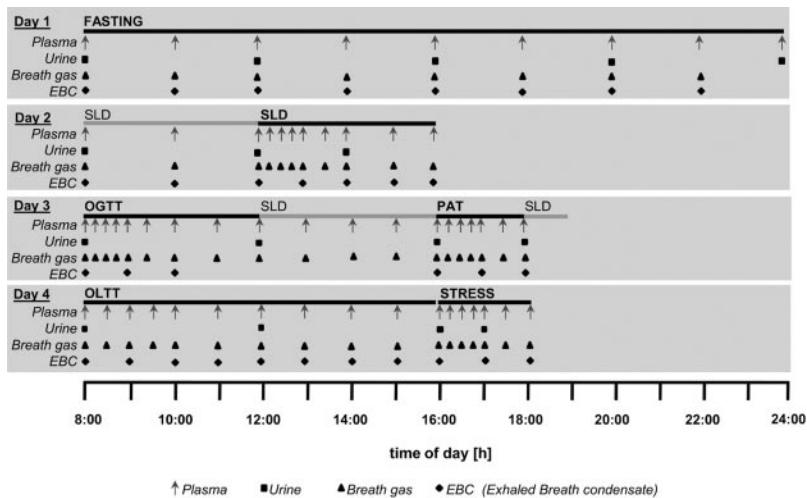
Figure 1. Study design of the HuMet study. Within 4 d, volunteers underwent the 6 challenges: fasting, SLD, OGTT, PAT, OLTT, and stress (cold stress test). Solid bars indicate duration of each challenge test. Symbols indicate time points of biofluid collection.

RMR multiplied by a factor of 1.3 for low physical activity. Samples were always taken shortly before each challenge test (0 min) and then at predefined time points.

Fasting challenge

After the evening meal at 7 PM on d 1, the study participants fasted until 8 AM the next morning, when the first samples were obtained, and then continued fasting for another 24 h. Plasma and breath air samples were collected every 2 h between 8 AM and midnight and again after a total fasting period of 36 h. Urine was collected every 4 h between 8 AM and midnight and again after 36 h of fasting. EBC was collected every 2 h between 8 AM and 10 PM and again after a total fasting period of 36 h. During the fasting period, subjects received 2.7 L of mineral water according to a predefined drinking schedule.

SLD challenge

To investigate the effects of a complex, balanced diet, subjects received a highly defined fiber-free formula drink (Fresubin Energy Drink, chocolate flavor), providing 1/3 of the individual daily energy requirements, at noon on d 2 for ingestion within 5 min. Plasma and exhaled air were collected at 0, 15, 30, 45, 60, 90, 120, 180, and 240 min. EBC was collected at 0, 60, 120, 180, and 240 min. Urine was collected at 0 and 120 min.

OGTT challenge

On d 3, an OGTT was carried out at 8 AM after an overnight fast by ingesting 75 g of glucose drink (Dextro O.G.T.; Roche Diagnostics, Mannheim, Germany). All subjects were asked to drink the 300-ml glucose solution within 3 min. Plasma and exhaled air samples were collected at 0, 15, 30, 45, 60, 90, 120, 180, and 240 min. EBC was collected at 0, 60, and 120 min. Urine was collected at 0 and 240 min.

PAT challenge

All subjects performed a 30-min bicycle ergometer training at a power level corresponding to their individual anaerobic threshold. Plasma and exhaled air was obtained before the PAT, during the PAT at 15 and 30 min, and after the PAT at 45, 60, 90, and 120 min. EBC collections were performed at 0, 60 and 120 min. Urine was collected at 0 and 120 min.

OLTT challenge

The lipid-rich liquid test diet consisted of 3 parts Fresubin Energy Drink and 1 part Calogen (Nutricia, Zoetemeer, The Netherlands), a fat emulsion containing 50 g of long-chain triglycerides per 100 ml. The volume of the liquid meal was calculated for each volunteer to provide 35 g fat/m^2 body surface area. The test drink was served at room temperature for ingestion within 5 min. Plasma and exhaled air samples were collected at 0, 30, 60, 90, and 120 min and thereafter every hour until 8 h after lipid ingestion. EBC was sampled at 8 AM (0 min) and then every hour after the OLTT until 4 PM (480 min). Urine was collected at 0, 4, and 8 h. The compositions of all liquid diets are provided in Supplemental Table S1.

Stress challenge

To elicit a hormonal stress response and examine its effect on metabolism, volunteers underwent a cold pressure test by immersing one hand, up to wrist level, with fingers apart, for maximal 3 min in ice water. Plasma and exhaled air samples were obtained at 0, 15, 30 45, 60, 90, and 120 min. Urine and EBC were collected at 0 and 60 min.

Sample collection

Plasma

During the study, a total of 56 blood samples/subject were collected into 9-ml EDTA K$_2$-Gel tubes (Sarstedt, Nümbrecht, Germany) through a venous cannula (18-gauge 1¾; Vasofix Braunüle, Braun, Germany) inserted into an antecubital vein. Tubes were mixed and centrifuged immediately (5702 R centrifuge; Eppendorf AG, Hamburg, Germany) at 3000 g for 10 min at 20°C. Obtained plasma was immediately portioned into aliquots, frozen on dry ice, and subsequently stored at −80°C until further analysis.

Urine

Spot urine samples were collected into 125-ml polypropylene beakers (Ratiolab, Dreieich, Germany), immediately portioned into aliquots, frozen on dry ice, and then stored at −80°C until analysis.

Breath air

The exhaled breath samples were collected into reusable 3-L polytetrafluoroethylene (Teflon) bags (SKC, Eighty Four, PA, USA) using the mixed expired sampling technique. Subjects filled the bag in a single exhalation. Breath gas collection was scheduled immediately before each blood collection. Room air was drawn contemporaneously. Breath and room air were sampled at the test location and analyzed immediately by proton transfer reaction (PTR)-MS. Before PTR-MS analysis, the filled bags were heated up in an oven for ≥5 min at 40°C in order to evaporate the condensed humidity.

EBC

EBC was sampled using an ECO Screen II condenser (Jaeger GmbH, Hoechberg, Germany). Therefore, subjects respired into the device for ~10 min to collect 150 l breath volume. EBC was collected into two cooled (−20°C) disposable polytetrafluoroethylene plastic bags. The exhaled air is fractioned into bronchial and alveolar breath partitions, each collected into one of the two cooled bags. Samples were immediately transferred into 1.5-ml storage tubes, frozen on dry ice, and stored at −80°C until measurement.

Standard biochemistry parameters

Venous plasma glucose and lactate concentrations were determined by enzymatic amperometric technique (Super GL easy$^+$; Dr. Müller Geräte Bau, Freital, Germany). Insulin was measured by enzyme-linked immunosorbent assay (ELISA; K6219; Dako, Glostrup, Denmark). Nonesterified fatty acids (NEFAs) were quantified in plasma by an enzymatic colorimetric method (NEFA-HR; Wako Chemicals GmbH, Neuss, Germany) according to the manufacturer's recommendations.

Metabolomics analyses

Targeted metabolomics

Flow injection analysis (FIA)-MS/MS-based analysis using the AbsoluteIDQ kit (Biocrates Life Sciences AG, Innsbruck, Austria) was performed as described previously (9–11) by using a 4000 QTRAP system (AB Sciex, Darmstadt, Germany). The metabolomics data set contains 14 amino acids; hexose; free carnitine (C0); 40 acylcarnitines, hydroxylacylcarnitines, and dicarboxylacylcarnitines; 15 sphingomyelins; 77 phosphatidylcholines; and 15 lysophosphatidylcholines. Data quality was assessed by repeated measurements of the same sample (5×) on different days. Metabolites showing a coefficient of variation (CV) > 25%, as well as metabolites with CV > 20% and a significant correlation (Kendall) to the run day, were excluded from further analysis.

NMR metabolomics in plasma

Lipoproteins were analyzed by NMR spectroscopy at LipoFIT Analytic GmbH (Regensburg, Germany). The technology was patented (U.S. 7,927,878; Australia 2005250571; Germany 10 2004 026 903 B4). Briefly, diffusion-weighted NMR spectra of blood plasma were recorded on a Bruker Avance II^{plus} 600-MHz spectrometer (Bruker Daltonics, Bremen, Germany), which revealed characteristic overall profiles of the lipoprotein signals. The spectral regions of the spectra ranging from 1.5 to 0.7 ppm were modeled into a set of 15 lipoprotein subfractions. These 15 lipoprotein subfractions

were used to calculate lipoprotein size and quantity (number) in terms of the concentration (nM) of particle subclasses and the average particle size (nm).

NMR metabolomics in urine

NMR spectroscopy was carried out at LipoFIT Analytic on a Bruker Avance II^{plus} 600-MHz spectrometer. We recorded 1-dimensional ^{1}H-NMR NOESY experiments from the urine specimen in phosphate buffer at pH 7.4 with 1,1,2,2-tetra-deutero-3-trimethylsilylpropionic acid (TSP) for reference at a frequency of 600.30 MHz. Metabolites in these NMR spectra were annotated using the Chenomx NMR Suite 7.0 (Chenomx Inc., Edmonton, AB, Canada; ref. 12). Metabolite assignment was done manually since varying sample conditions affect the chemical shift of the metabolite resonances. The signal of a reference compound added to the specimen (TSP, 0.5 mM) was used to determine absolute metabolite concentrations. We normalized these concentrations by urinary creatinine levels and report them as millimoles per mole of creatinine.

Nominal mass PTR-MS metabolomics in breath air

From every breath sample, 5 mass scans in the mass range between 20 and 200 amu were recorded with a standard PTR mass spectrometer (Ionicon, Innsbruck, Austria). The recorded counts of every mass were normalized to the count rate of the primaries and water clusters to compensate for fluctuations in the primary concentrations and for consumption of the primary ions in saturated breath gas compared to the drier room air. Because of the extraordinary high increase of the acetone count rate during the elongated fasting period, the acetone count rate was additionally factored into the normalization. The change of transmission of the PTR mass spectrometer over time was corrected, and the conversion of the normalized count rate to parts per billion volume (ppbv) used the standard formula for PTR-MS concentrations (13). Masses were excluded from comparison if normalized count rates were below 2 normalized counts/s in 80% of the data points of a challenge. Due to the unit mass resolution of the PTR mass spectrometer, the assignment of a mass to a specific compound is rather tentative. However, in the selected cases, the linear correlation between the isotope count rates supported the assignment (*e.g.*, acetone).

Flow injection electrospray ionization ion cyclotron resonance Fourier transform (FIESI-ICR-FT)/MS nontargeted metabolomics

Samples were measured at Helmholtz Zentrum München using a Bruker Solarix FT-ICR mass spectrometer (Bruker Daltonics, Bremen, Germany) with a 12-T magnet and an Apollo II electrospray ionization source. Ionization was performed at positive mode and voltage of 4500 V. Samples were flow injected at 2 μl/min flow rate. In total, 420 time-domain transients were acquired and accumulated per sample. Each Fourier-transformed mass spectrum consists of 2 megaword data points, resulting in a mass resolving power of 400,000 at m/z 200 and 200,000 at m/z 400. Prior to analysis, mass spectra were calibrated with an error of <100 ppb using arginine clusters. Further calibration and mass spectrum unification was performed as described previously (14). Masses were filtered with a signal to noise ratio of 4 and/or 10^{-6}% of maximum intensity. Masses were annotated using the MassTRIX server (15) at 0.5 ppm accuracy. Unified spectra were normalized on the sum of signal intensities per spectrum and then subject-wise on the sum of normalized

signal intensities, to compensate for different ion strengths in samples and for interindividual variation, respectively.

Statistical analysis

Principle component analysis (PCA) For unsupervised multivariate data analysis, we performed PCAs using the *prcomp* function as implemented in the R 2.10.1 statistical software (http://www.r-project.org). The analyses were based on the quantitative data for all metabolic traits in plasma (132 by FIA-MS/MS, 28 by NMR, 3 by standard biochemistry). On the one hand, we determined the principal components of the mean concentrations of the 15 subjects at the 56 plasma sampling time points (56×163 data matrix). On the other hand, we performed a PCA on the complete data matrix for plasma (840×163). To this end, we first excluded rows (samples) with >80% missing values (23) and imputed the remaining missing values according to the following rules: if missing, the value for the data point $q_{metab,subject,t}$ is set to the mean of $q_{metab,subject,t-1}$ and $q_{metab,subject,t+1}$, whenever $q_{metab,subject,t-1}$ and $q_{metab,subject,t+1}$ are nonmissing values. Otherwise, a missing value for $q_{metab,subject,t}$ is replaced by the mean value $qmean_{metab,t}$ for the time point t over all subjects. For the PCAs, each metabolite column of the respective data matrix was scaled to a mean of 0 and a standard deviation of 1 in order to make the concentrations comparable.

Pearson correlation For 275 metabolites (163 in plasma, 106 in breath air, 6 in urine), we calculated the mean concentrations of the 15 subjects at the 56 plasma sampling time points, resulting in a mean time course for each metabolite. For metabolites quantified with the AbsoluteIDQ kit, log-transformed values were used, because most metabolite concentrations showed a log-normal distribution. Pearson correlations between metabolite mean time courses were calculated in order to uncover metabolites with similar or opposed time curves. The Pearson correlation coefficients were determined using the *cor.test* function in R. The matrix of pairwise Pearson correlation coefficients was hierarchically clustered and color-coded using the *heatmap* function with the default values for the clustering.

In general, metabolite quantities are provided as means ± SD.

Mathematical modeling of fatty acid β-oxidation

The fatty acid β-oxidation was described as a linear cascade of subsequent, irreversible first-order reactions such as $\dot{M}_i(t) = k_{i-1}(t) \cdot M_{i-1}(t) - k_i(t) \cdot M_i(t)$, with $\dot{M}_i$ being the time derivative dM_i/dt and k_i and k_{i-1} conversion rate parameters. The change of a metabolite M_i in the cascade at time t thus depends on the production of M_i by shortening of M_{i-1} (first part on the right-hand side of the equation) and the conversion of M_i to M_{i+1} (second part). For a more detailed description of the model, see Supplemental Data. All reactions were described in this fashion and combined to a system of differential equations. Solving this system for steady-state conditions (*i.e.*, metabolite concentrations do not change over time) yields conversion rates that are proportional to concentration ratios, also referred to as model-driven ratios. The correlations between anthropometric and biochemical parameters, such as BMI or plasma glucose, with metabolite concentrations and model-driven ratios were calculated with Spearman's rank correlation statistics. Rank correlations for biochemical parameters were calculated using metabolite concentrations of the fasting period. Anthropometric parameters were correlated with averaged metabolite concentrations of the fasting period. P values were corrected for multiple testing by controlling the false discovery rate at a global significance level of 0.05 (16). P_{gain} statistics for metabolite ratios were calculated as:

$$P_{gain}\left(\frac{M_1}{M_2}, X\right) = \frac{\min\left(P(M_1, X),\, P(M_2, X)\right)}{P\left(M_1 / M_2, X\right)}$$

with metabolites M_1 and M_2 and their respective model-driven ratio M_1/M_2, parameter X (*e.g.*, BMI) and $P(A, B)$ being the corrected P value of Spearman's rank correlation between variable A and variable B. For cases where the model improves statistical correlations, values of P_{gain} will be >1. All analysis steps were performed using Matlab 7.11 (MathWorks, Natick, MA, USA).

RESULTS

Time-dependent metabolite changes reflect the metabolic conditions induced by the challenges

The challenges performed within this study induced either anabolic or catabolic states, resulting in reversible metabolite changes. As expected, plasma concentrations of glucose and insulin were constantly low during fasting (85.9 ± 11.3 mg/dl and 4.6 ± 1.5 μIU/ml) and increased 30 min after the OGTT (141.8 ± 28.6 mg/dl and 48.8 ± 21.3 μIU/ml). Plasma lactate levels showed the most prominent increase within 30 min of intensive cycling (PAT; from 9.6 ± 2.9 to 66.5 ± 25.7 mg/dl, change$=+595\%$). Fasting for 36 h increased NEFAs and branched chain amino acids in plasma, acetone in urine and breath, and, interestingly, also urinary excretion of β-aminoisobutyrate (**Fig. 2**). Complementary EBC profiles of putatively annotated m/z peaks showed a decrease in concentrations of medium oxoacids, such as oxodecanoic acid ($[C_{10}H_{18}O_3 + Na]^+$, $\Delta m/z = 0.024$ ppm) and oxododecanoic acid ($[C_{12}H_{22}O_3 + Na]^+$, $\Delta m/z = -0.065$ ppm). Oxoacids are implicated in fatty acid biosynthesis. To investigate similarities in the time courses of metabolites, we provided a pair-wise cross-correlation analysis of 275 metabolites quantified in plasma, urine, and breath air in samples of all time points (**Fig. 3**). High positive correlations (shown in red in Fig. 3) indicate metabolites with coherent concentration changes over time. High positive correlations ($r=0.94$, $P<2\times10^{-16}$) were found between metabolites such as glucose and hexoses measured by different methods, or between metabolites that are known to be biochemically interconnected, such as chylomicron and VLDL quantity ($r=0.9$, $P<2\times10^{-16}$). Insulin was positively correlated with anabolic metabolites, such as glucose ($r=0.88$, $P<2\times10^{-16}$) but also revealed high correlations with C0 ($r=0.69$, $P=5.1\times10^{-9}$), propionylcarnitine (C3; $r=0.71$, $P=1.0\times10^{-9}$) or proline ($r=0.68$, $P=7.8\times10^{-9}$). C0 was positively correlated with the short-chain acylcarnitines, especially C3 ($r=0.71$, $P=7.4\times10^{-10}$) and valerylcarnitine (C5; $r=0.67$, $P=1.4\times10^{-8}$), but negatively with longer acylcarnitines and acetylcarnitine (C2), which showed the strongest anti-correlation ($r=-0.7$, $P=2.1\times10^{-9}$). Over the 36 h of fasting, C2 levels increased from 5.4 ± 1.1 to 15.9 ± 5.0 μM, whereas C0 decreased from 39.7 ± 7.2 (basal) to 33.9 ± 8.2 μM. **Figure 4A** illustrates the mirror-like anticorrelation ($r=-0.66$, $P=2.4\times10^{-8}$) of circulating
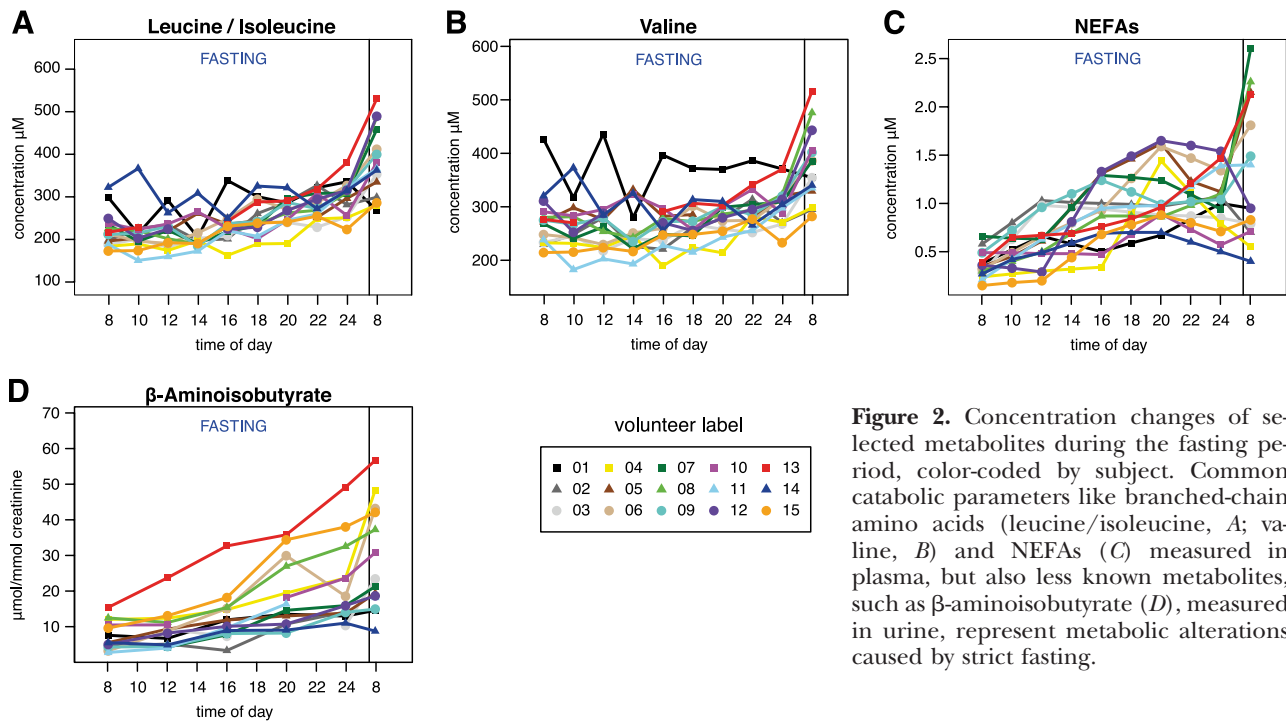
Figure 2. Concentration changes of selected metabolites during the fasting period, color-coded by subject. Common catabolic parameters like branched-chain amino acids (leucine/isoleucine, *A*; valine, *B*) and NEFAs (*C*) measured in plasma, but also less known metabolites, such as β-aminoisobutyrate (*D*), measured in urine, represent metabolic alterations caused by strict fasting.

plasma levels of C0 and the sum of acylcarnitines over all time points and challenges.

Readouts for the metabolic condition were also derived by multivariate data analysis on the entire metabolite profiles in plasma. PCA performed over all time points revealed distinct time-dependent trajectories of the metabolic profiles, reflecting the different metabolic conditions during the challenges. This was particularly apparent for the exercise challenge. As highlighted in Fig. 4*B*, excursion of the metabolite profiles began immediately after starting the 30-min cycling exercise, and within only 2 h, the metabolite fingerprints returned almost to the original location.

Interindividual variation during challenges

Baseline anthropometric and routine clinical data are provided in **Table 1**. Our study cohort consisted of 15 healthy, male Caucasians with similar BMI (23.1 ± 1.8 kg/m^2) and age (27.8 ± 2.9 yr). **Figure 5*A*** demonstrates that the difference between subjects in plasma concentration of a metabolic parameter was markedly increased or decreased by a metabolic challenge. For anabolic parameters, such as glucose or insulin, this distance was enlarged in postprandial states, *e.g.*, after the OGTT, SLD, and OLTT, whereas concentrations were very stable and showed little variation between the volunteers during the 36 h of fasting. In contrast, the fasting caused the most pronounced between-subject differences in catabolic metabolites. For example, the increase in plasma C2 after 36 h fasting was accompanied by an elevated coefficient of variation (31.6%) when compared to baseline (20.5%). The increase of interindividual variation in catabolic metabolites during fasting was observable in all sample types (Fig. 5*B*). Figure 5*B* also shows that volunteer 13

(V13, red) and volunteer 14 (V14, dark blue) marked the extremes of plasma C2 concentration changes within the study cohort. The plasma C2 concentration of V13 was >3-fold higher (25.8 μM) at the end of the fasting period than that of Vl4 (8.1 μM). Interestingly, these different responses to the fasting state spanned across other catabolic marker metabolites, such as acetone in urine and breath, as evident by the consistent position of the subjects in the time-concentration profiles. V13 showed all indicators of a strong fasting response, with enhanced levels of plasma NEFAs and highest β-aminoisobutyrate in urine of our cohort (Fig. 2). In contrast, V14 showed the lowest levels in all these fasting-state metabolites of different sample types. A PCA (Fig. 5*C*) performed over all plasma samples (*i.e.*, all subjects at all time points) with samples colored by subject showed that the samples of each subject were grouped together when transformed to the first 3 principal components (PC1, PC2, and PC3). This grouping was evident over all time points and even more distinct if only samples of the 36-h fasting period are shown. The relative contribution (loadings) of individual metabolites in the PC1–PC3 dimensions are provided in Supplemental Fig. S1.

Readouts from a β-oxidation model provide stronger associations with phenotypic data than absolute metabolite concentrations

V13 and V14 showed marked differences in the responses to the fasting challenge. We assumed that those differences could be associated with the volunteers' muscle or fat mass, expecting that higher fat mass should correspond with a higher plasma concentration of NEFAs, resulting in higher ketone body production in the catabolic condition. However, V13 and V14 were
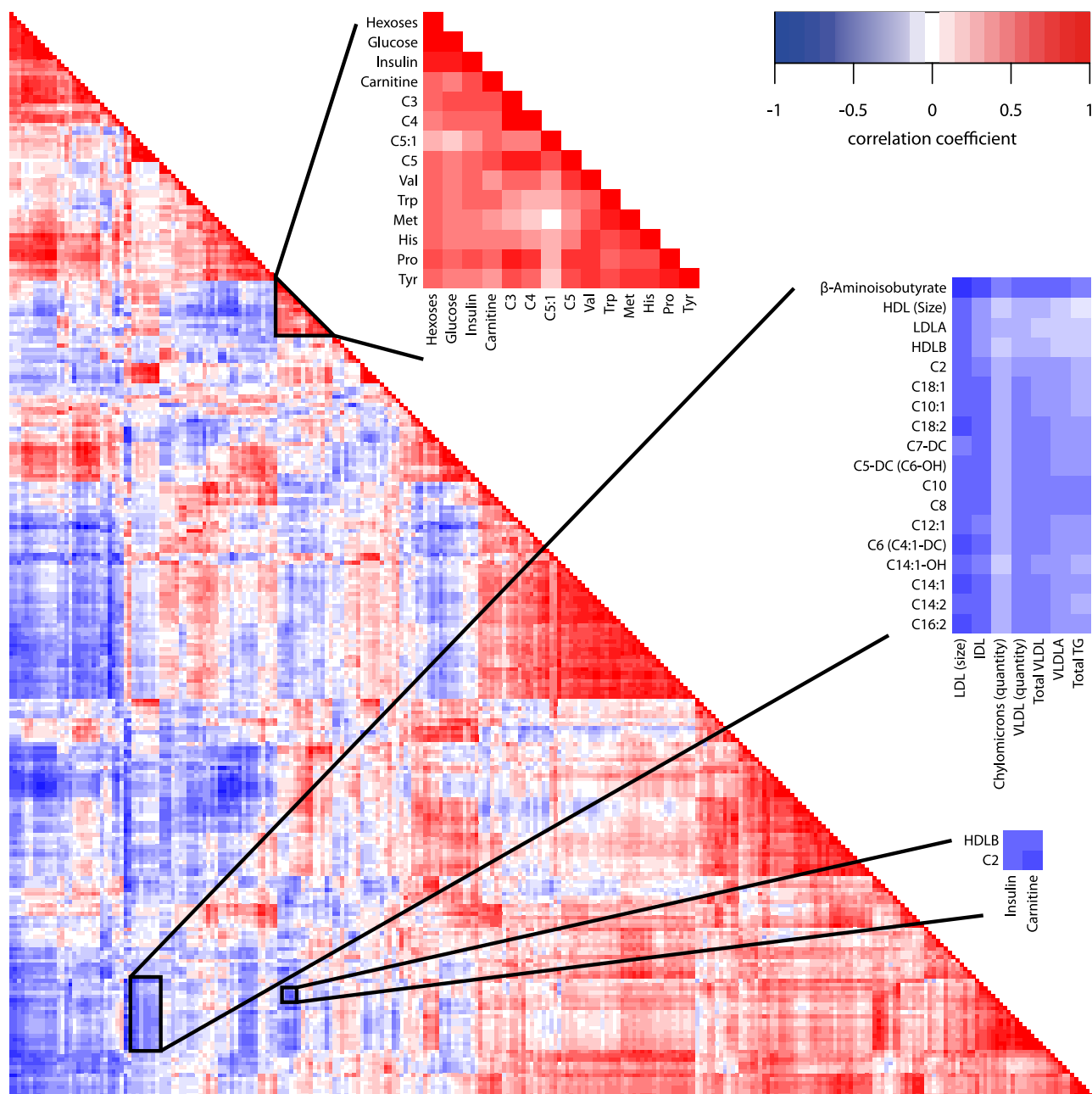
     KRUG *ET AL.*

Figure 3. Correlations in metabolite trends. Pearson's correlations of 275 metabolites, measured in plasma (163 metabolites), urine (6 metabolites) and breath air (106 metabolites). Cross-correlation of mean time courses of each metabolic trait reveals metabolites with a similar or opposite trend in their concentration curves. High positive correlations indicate similar behavior with regard to the direction of change induced by the challenge protocol. Zooming into panels reveals correlated (red) or anticorrelated (blue) metabolites.

similar in their anthropometric measures, such as BMI (22.8 *vs.* 25.1 kg/m^2) or RMR (1710 *vs.* 1850 kcal). A correlation analysis revealed no or only weak correlations between metabolite concentrations and anthropometric measures in our study cohort. Therefore, we hypothesized that the individual's metabolic capacity in utilization of fatty acids might provide an explanation for the disparate responses to the fasting condition.

Consequently, we developed a simplified mathematical model of the fatty acid β-oxidation cascade. As input variables, we used plasma acylcarnitines of different chain lengths as proxies for β-oxidation intermedi-

ates during the 36 h of fasting. The readouts of our modeling process are estimated reaction rate parameters, which can be proportionally described by ratios between acylcarnitines. As presented in **Table 2**, especially the ratio C2/C16 provided stronger correlations with anthropometric measures (*e.g.*, BMI, fat mass or muscle-fat-ratio) than absolute plasma concentrations of C2 or C16. The model-driven ratio therefore improved statistical correlations, expressed as values of $P_{gain} > 1$, yielding, for example, 8.8 for correlation with BMI, 7.3 for muscle-fat ratio, and up to 18 for total fat mass. In some cases, only model-driven ratios were
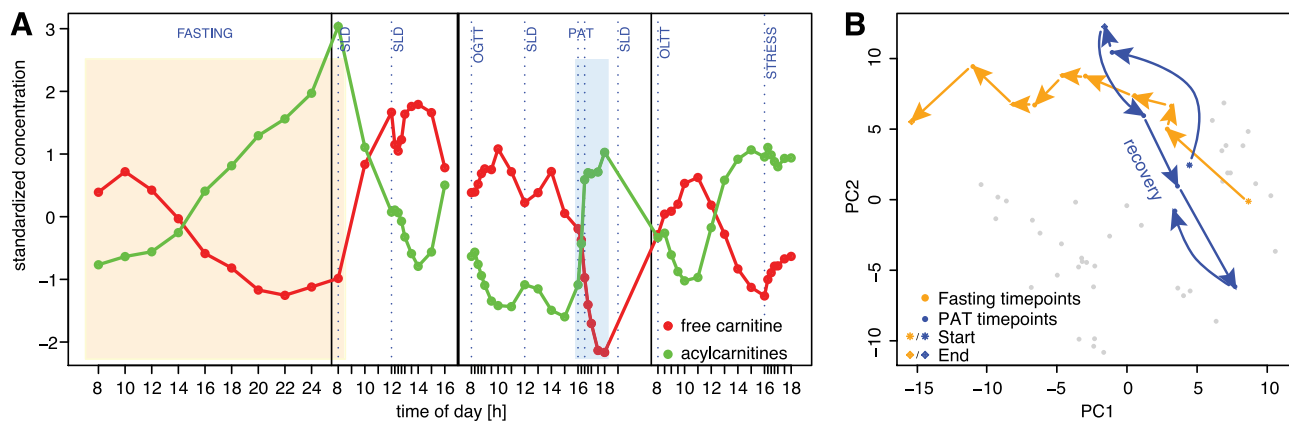
Figure 4. Metabolic response to challenges. *A*) Mean plasma concentrations of the 15 subjects at each sampling time point of C0 (red) and the sum of all acylcarnitines including C2 (green) are significantly anticorrelated ($r=-0.66$, $P=2.4\times10^{-8}$), reflecting switches between anabolic and catabolic metabolism induced by the various challenges. For better visualization, respective mean concentrations were scaled to a mean $\pm$ sd of 0 ± 1. *B*) PCA is based on the metabolic profiles of all time points in plasma (56×163 data matrix, see Materials and Methods). PAT challenge time points (blue) started at 4 PM with sampling at 0, 15, and 30 min during cycling and in the recovery phase at 15, 30, 60, and 90 min after cycling. Time points of the fasting challenge (orange) started with a sample taken at 8 AM (after an overnight fast), followed by samples taken after further 2, 4, 6, 8, 10, 12, 14, 16, and 24 h. According to the different challenges, the samples are located in a time-dependent trajectory in the metabolic space spanned by the first 2 principal components (PC1 and PC2).

significantly correlated with anthropometric parameters (underscored values in Table 2). Biochemical parameters, such as fasting glucose or insulin levels, also revealed higher correlation coefficients with model-derived ratios than with the absolute plasma levels, for example, of acylcarnitines (Table 2 and Supplemental Fig. S2).

TABLE 1. *Baseline anthropometry and blood chemistry of the study cohort*

Parameter	Mean $\pm$ sd	CV (%)
	Value	
Age (yr)	27.8 $\pm$ 2.9	10.7
Height (m)	1.8 $\pm$ 0.1	3.5
Weight (kg)	77.5 $\pm$ 7.1	9.1
BMI (kg/m^2)	23.1 $\pm$ 1.8	7.6
FM (kg)	14.4 $\pm$ 3.3	23.1
FFM (kg)	59.5 $\pm$ 5.9	9.9
Waist circumference (cm)	80.5 $\pm$ 4.6	5.7
Hip circumference (cm)	90.1 $\pm$ 4.7	5.2
Heart rate (min^{-1})	62 $\pm$ 11.4	18.4
Blood pressure, systolic (mmHg)	118.8 $\pm$ 5.9	4.9
Blood pressure, diastolic (mmHg)	81.9 $\pm$ 5.9	7.3
24 h RMR (kcal)	1721.3 $\pm$ 223.6	13
RQ	0.85 $\pm$ 0.1	6.5
Total cholesterol (mg/dl)	169.8 $\pm$ 37.5	22.1
Triglycerides (mg/dl)	78.1 $\pm$ 26.2	26.2
Lactate (mg/dl)	9.6 $\pm$ 2.9	29
Glucose (mg/dl)	84.9 $\pm$ 7.5	8.8
Insulin (μIU/ml)	5.7 $\pm$ 1.4	23.6

Values were measured after a 12-h overnight fast (n=15). BMI, body mass index; FM, fat mass; FFM fat free mass; RMR, resting metabolic rate; RQ, respiratory quotient; CV, coefficient of variation.

DISCUSSION

Metabolite changes reflect the challenges

The human metabolome is subject to continuous changes. Anabolic conditions, as after food intake, and catabolic states during fasting or physical exercise are an expression of the plasticity of metabolic control. Here, we present a study that conceptually explores the metabolic plasticity by analyzing metabolite changes in response to 6 metabolic challenges stimulating either catabolic conditions (fasting and cycling) or anabolic states (OGTT, OLTT, and SLD). According to the catabolic to anabolic shifts and *vice versa*, the plasma concentrations of standard parameters like insulin, glucose, and lactate revealed the expected alterations, demonstrating the validity of the applied challenges and the acquired data set. As insulin drives the transition from a fasting state to a fed state, its time course was positively correlated with anabolic metabolites, such as glucose, but also revealed less known correlations over time with C0 and the short-chain acylcarnitines C3, C4, and C5. During fasting, increased lipolysis and β-oxidation of fatty acids in mitochondria provides most of the energy needed. Fatty acids enter the cytosol from plasma, are converted into CoA-thioesters, and subsequently are transferred into the mitochondria *via* the palmitoyl-CoA carnitine transferase II shuttle (17, 18). Since this acyl-CoA import requires C0, the decline in plasma C0 concentrations during fasting observed here indicates that the cellular carnitine supply is increased by its uptake from plasma. Moreover, it has been hypothesized previously that a spillover of acetyl- and acyl-CoA due to increased fatty acid flux through β-oxidation in cells is buffered by releasing the respective carnitines into plasma
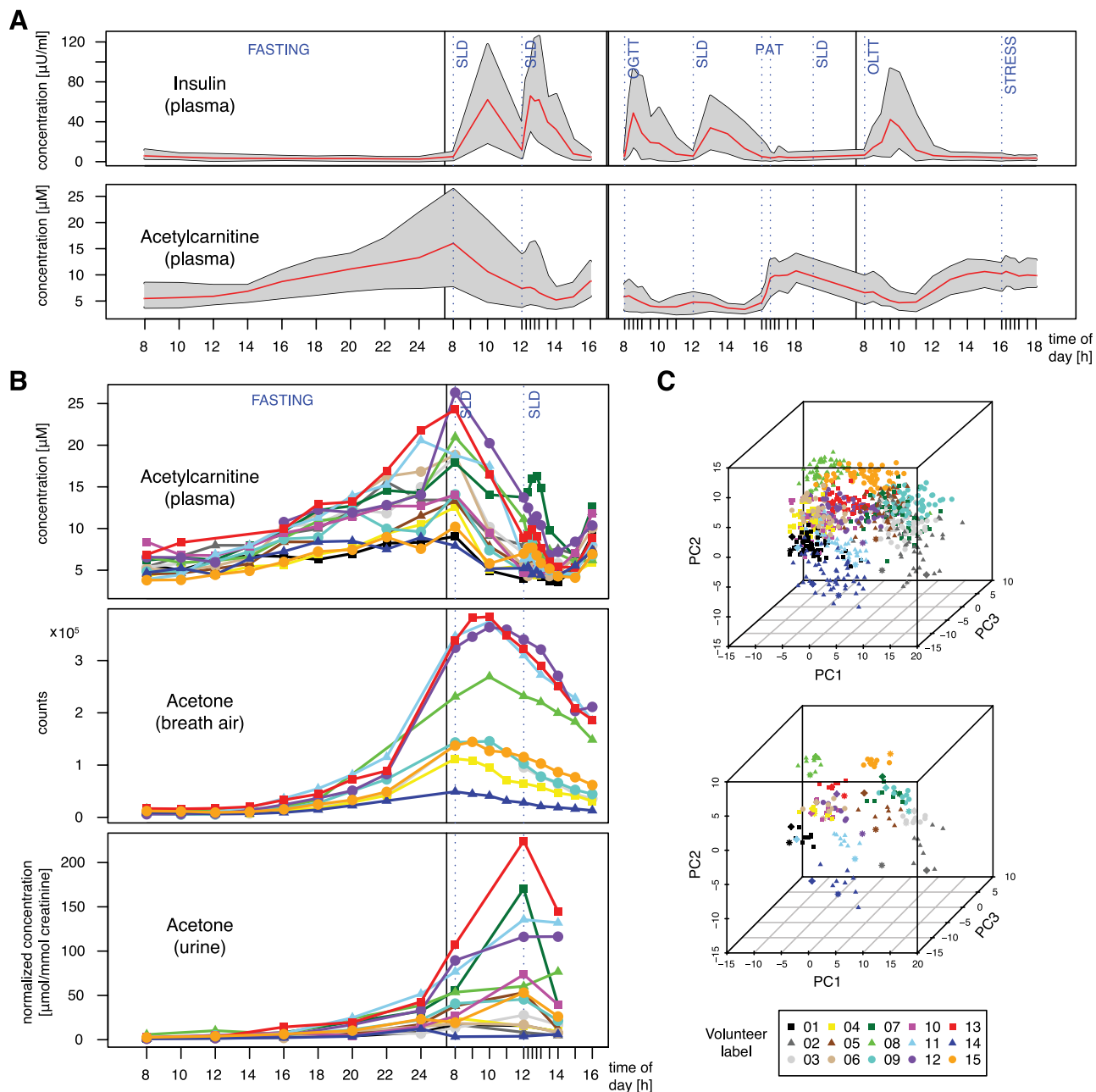
Figure 5. Interindividual variation of metabolite concentrations in the context of challenges and sample types. *A*) Depending on the challenges, the interindividual variation in the concentrations of metabolites increased or decreased. Mean plasma concentrations of insulin and C2 are shown as red curves. Shaded area denotes the between subject-distance, *i.e.*, the range between the minimal and the maximal concentration observed in any participant. *B*) For d 1 and d 2, the individual C2 concentration curves in plasma are shown for each subject (top panel). The quantities of acetone in breath air (determined by PTR-MS; middle panel) and urine (determined by NMR; bottom panel) match the observations seen for C2 (determined by MS/MS) in plasma. The large differences in the concentrations between subject 14 and subject 13 are consistent across the 3 sample types. *C*) Top panel: score plot of a PCA based on the metabolic profiles of all samples in plasma (840×163 data matrix, see Materials and Methods). Bottom panel: PCA plot including only samples of the fasting challenge. Despite intraindividual variations due to various challenges and sampling times, the samples of each subject are grouped together by the PCA using only the principal components 1–3 (PC1–PC3).

(19, 20). Our results are consistent with this view, as plasma levels of C2 and all acylcarnitines, except C3, C4, and C5, showed a strong increase in times of elevated β-oxidation, *e.g.*, during fasting or exercise. When catabolism was reversed to an anabolic state with elevated plasma insulin levels, the exact opposite effect on the levels of C0 and C2 or the sum of

acylcarnitines was observed. Therefore, the circulating plasma levels of C0 and the sum of acylcarnitines responded in an almost mirror-like anticorrelation to catabolic and anabolic challenges. The mirror-like anticorrelation of C0 *vs.* C2 was observed over the entire 4 d of the trial and suggests that these two metabolites or their ratio may serve as markers for

TABLE 2. *Model-derived metabolite ratios improve correlation with metabolic parameters*

| | | | Rank correlation | | | | | |
| | | | C2/Cx vs. ABP | | C2 vs. ABP | | Cx vs. ABP | |
P_{gain}	Cx	ABP	P	ρ	P	ρ	P	ρ
7.5×10^6	C16	Sum of hexoses (p)	1.9×10^{-15}	−0.61	1.4×10^{-8}	−0.48	0.632	0.07
3.5×10^5	C16	β-Aminoiso-butyrate (u)	1.6×10^{-16}	0.77	5.7×10^{-11}	0.67	0.901	0.03
2.9×10^3	C6[a]	Free carnitine (p)	5.1×10^{-7}	−0.41	0.001	−0.29	0.918	0.02
221.5	C18	Glucose (p)	1.4×10^{-5}	−0.46	0.003	−0.35	0.520	0.11
87.1	C4	Free carnitine (p)	2.5×10^{-6}	−0.39	0.001	−0.29	2.1×10^{-4}	0.33
51.4	C18	Hydroxyliso-butyrate (u)	4.1×10^{-9}	0.59	2.1×10^{-7}	0.55	0.914	0.03
18.1	C16	Fat mass	<u>0.015</u>	−0.68	0.731	−0.19	0.267	0.44
10.9	C18	Creatinine (p)	<u>0.028</u>	−0.62	0.405	−0.35	0.301	0.42
8.8	C16	BMI	0.002	−0.77	0.944	−0.04	0.014	0.70
8.5	C16	Body fat percentage	<u>0.042</u>	−0.58	0.798	−0.14	0.354	0.39
7.3	C16	Muscle-fat-ratio	<u>0.037</u>	0.60	0.850	0.11	0.271	−0.43
5.3	C4	Insulin (p)	<u>0.018</u>	−0.28	0.093	−0.23	0.200	0.19

Correlations between anthropometric and biochemical parameters (ABPs) with metabolite concentrations (C4, C6, C16, C18, and C2) and model-driven ratios derived from the β-oxidation model. Biochemical parameters and acylcarnitine and C2 concentrations were measured during the fasting period of study day 1. Rank correlation *P* values were corrected for multiple testing using FDR at global significance level of 0.05. Underscored values indicate cases for which only model-driven ratios, but not single metabolite levels, were significantly correlated with ABPs. Model-driven ratios reflecting biological processes improve statistical correlations with ABPs of energy metabolism when compared to the correlations with single metabolite concentrations, resulting in values of $P_{gain} > 1$. Cx, acylcarnitine with chain length *x*; ρ, Spearman's rank correlation coefficient; p, parameter concentration determined in blood plasma; u, parameter concentration determined in urine. [a]Detection methods cannot distinguish between C6 and C4:1-DC.

any shift from catabolic to anabolic state and *vice versa.*

Anabolic and catabolic states of metabolism were also obvious in a PCA performed over all time points that revealed distinct time-dependent trajectories of the metabolic profiles. Therefore, these trajectories reflect the plasticity of the metabolite profile by illustrating metabolite alterations induced by the challenges and the return to the initial situation.

Interindividual variation can be extended and compressed by metabolic challenges: the accordion effect

Recognizing that the human metabolome is influenced by a number of factors, strict subject inclusion criteria were met in the present study. As intended, the study participants consisted of a homogeneous group (Table 1) of 15 healthy, male Caucasians within a narrow BMI and age range. Sample collection, processing, and subject treatment were also highly standardized to minimize variation. Despite best possible standardization, our metabolome data demonstrated between-subject variation, probably originating from environmental conditioning (dietary habits, lifestyle, *etc.*) on basis of a given genetic/epigenetic makeup. A PCA of all plasma metabolites showed that despite large intraindividual variation over the various challenges, the samples of each subject were clustered together. This was even more pronounced after a strong metabolic challenge, such as a 36-h fasting period. Regarding the individual time courses of the measured parameters, we observed that the intersubject variation of a metabolic parameter was markedly increased or decreased by a

metabolic challenge, even in volunteers of otherwise similar phenotypic appearance. For anabolic parameters, such as glucose or insulin, the distance between subject concentrations was enlarged in postprandial states, *e.g.*, after the OGTT, SLD, and OLTT, whereas the concentrations were very stable and showed little variation between the volunteers during the 36 h fasting. In contrast, the fasting caused the most pronounced differences between subjects in catabolic metabolites, *e.g.*, C2 in plasma or acetone in urine and breath. The elevation in interindividual variation observed during the fasting challenge allowed identification of two distinct metabotypes, namely V13 and V14. Those two volunteers marked the extremes of the study cohort, as shown for the catabolic metabolites C2 in plasma or acetone in urine and breath (Fig. 5). V13 showed all indicators of a classical fasting response, with enhanced concentrations of plasma NEFAs as indicator of enhanced lipolysis, increased ketone body production with increased urinary excretion and exhalation in breath, and also highest urinary excretion of β-aminoisobutyrate (Fig. 2). β-Aminoisobutyrate is a thymine catabolite that was reported to increase fatty acid oxidation and reduce body fat in supplemented mice (21, 22). Our results indicate that β-aminoisobutyrate also provides a reliable marker for the degree of fatty acid oxidation in humans. In contrast, V14 appeared almost completely refractory to the catabolic condition with only small increases in fasting state metabolites and β-aminoisobutyrate in different sample types. This shows not only the high qualitative and quantitative consistency across samples from different body fluids and analysis platforms, but also

that it was possible to identify distinct metabotypes even in a homogenous cohort by differences in the responsiveness to challenges, such as extended fasting.

A model of β-oxidation provides parameters that correlate with the individual's metabolic condition

In search of the origin of the interindividual variation, especially in the fasting response, we performed a correlation analysis of metabolite concentrations and parameters derived from anthropometric measurements (body mass, fat and muscle mass, *etc.*), expecting that, for example, higher fat mass should correspond with higher NEFA or ketone body production during catabolic conditions. However, in our healthy, young cohort, the observed differences in metabolite concentrations during fasting provided no significant associations with anthropometric measures like body mass, fat, and muscle mass (Table 2). Therefore, we hypothesized that the individual's metabolic capacity in utilization of fatty acids might provide an explanation for the disparate responses to the fasting condition. Consequently, we asked whether model-derived parameters from a discrete biological process could provide a surrogate for metabolic differences. Since the true metabolic fluxes and their capacities are difficult to measure *in vivo*, we developed a simplified mathematical model for fatty acid β-oxidation. This model is based on the linearity and the irreversibility of the central reactions by which fatty acids released from adipose tissue during fasting are subsequently degraded in mitochondria. We used plasma acylcarnitines of different chain lengths with their characteristic changes during 36 h of fasting as input variables in our model, assuming that plasma acylcarnitines serve as proxies for intracellular β-oxidation intermediates. This assumption is supported by findings that inborn errors of β-oxidation lead to specific changes in plasma acylcarnitine levels (23, 24). Genome-wide association studies also reported robust statistical associations between plasma acylcarnitines and genetic variants of β-oxidation enzymes (10, 25). We therefore based our model on the acylcarnitines in plasma as representatives for β-oxidation intermediates.

With C18 as the initial substrate and C2 as the final product, a series of acylcarnitine ratios was derived from the model that correlated significantly with anthropometric parameters, such as BMI, total body fat mass, body fat content (%), or muscle-to-fat ratio (Table 2). Although C2 may, in small quantities, be derived from other sources than β-oxidation, the ratios derived from the acylcarnitines of different chain length can only represent fatty acid oxidation. These metabolite ratios as readouts of the simplified β-oxidation model appear to better describe individual metabolic capacities as compared to absolute concentrations of individual metabolites alone, since they inherently correct for individual variations of metabolite plasma levels. It also suggests that models based on biochemical knowledge can help to explain associations and variations among metabolite patterns, body composition, and metabolic state much better than absolute metabolite concentrations. Although the β-oxidation model has proven its feasibility by the coherence of the derived ratios with parameters that influence fasting-specific biochemical processes, there are some caveats. For example, the model assumes that the stepwise shortening of the fatty acid is irreversible under the given metabolic conditions, at least up to the last enzyme, which mediates the thiolytic cleavage. Moreover, fatty acid import into cells, as well as acylcarnitine efflux, should not be rate-limiting. The model also assumes steady-state conditions with capacity limits determined only by the available redox equivalents (FAD and NAD). When β-oxidation flux exceeds citric acid cycle and respiratory chain activity in muscle, hepatic ketone body production is increased. With a delay in time, this can easily be followed by enhanced excretion of acetone in breath and urine, as shown in our volunteers (Fig. 5B). Extending the β-oxidation model to ketone body production could further improve analysis of coherent changes in metabolome data sets. It seems valuable to apply such quantitative modeling approaches also to other metabolite data sets to obtain parameters that better reflect pathway capacities. These may help in the characterization of human metabotypes in genotype-phenotype association studies.

Perspectives: from healthy to disease states

Recent biomarker discovery studies based on metabolomics have identified plasma free fatty acids, acylcarnitines, ketone bodies, branched chain amino acids, and amino acid degradation products to be significantly altered in states of insulin resistance or diabetes type 2 (26–28). These putative metabolite biomarkers of a prediabetic or diabetic state strongly resemble the signature of metabolite changes of a prolonged fasting state (>20 h) in our healthy volunteers. In this respect, insulin-resistant or diabetic patients show metabolite profiles of a catabolic condition, even in an otherwise anabolic state. Increased ketoacid levels in urine or their volatile derivatives, such as acetone, found in breath characterized an advanced fasting state in our healthy volunteers and may in a postprandial condition report insulin resistance or diabetes-specific metabolic impairments that can easily be detected in noninvasive samples, such as urine or breath.

CONCLUSIONS

We have generated a large data set of time-dependent metabolite profiles representing normal and extreme metabolic conditions of young, healthy, male volunteers measured in different body compart-

ments and by a variety of state-of-the-art NMR- and MS-based methods. To our knowledge, this is the first time that all biochemical processes related to extended fasting, glucose and lipid tolerance tests, controlled meals, physical exercise, and physiological stress were explored in a single metabolome study. In an effort to describe the flexibility of the organismic response, we demonstrated an "accordion effect" for metabolite profiles, showing that challenges increase metabolite variability between volunteers, allowing discrete metabotypes to be identified that would not be seen in normal fasting conditions. Interindividual variability of selected metabolites was consistent across the studied sample types and emphasizes the potential diagnostic use of noninvasive samples, such as urine or breath. Plasma-free carnitine and acylcarnitines were shown to define best any catabolic and anabolic conditions and their transitions, and their ratio could be useful as marker for the metabolic state. These metabolites used as input and output variables in a quantitative systems biology model of β-oxidation revealed parameters that far better identify discriminators of the individual metabolic variation than absolute plasma concentrations, demonstrating that such modeling may aid in the interpretation of large metabolomics data sets. The freely available data set of the HuMet study provides a reference for future human studies and may also be used to develop and validate other metabolic models. ◾FJ◾

REFERENCES

1. Garrod, A. E. (1902) The incidence of alkaptonuria: a study in chemical individuality. [classic article] *Yale J. Biol. Med.* **75,** 221–231
2. Levy, P. A. (2010) An overview of newborn screening. *J. Dev. Behav. Pediatr.* **31,** 622–631
3. Jansson, J., Willing, B., Lucio, M., Fekete, A., Dicksved, J., Halfvarson, J., Tysk, C., and Schmitt-Kopplin, P. (2009) Metabolomics reveals metabolic biomarkers of Crohn's disease. *PLoS ONE* **4,** e6386
4. Bogdanov, M., Matson, W. R., Wang, L., Matson, T., Saunders-Pullman, R., Bressman, S. S., and Flint Beal, M. (2008) Metabolomic profiling to develop blood biomarkers for Parkinson's disease. *Brain* **131,** 389–396
5. Gowda, G. A. N., Zhang, S., Gu, H., Asiago, V., Shanaiah, N., and Raftery, D. (2008) Metabolomics-based methods for early disease diagnostics. *Expert Rev. Mol. Diagn.* **8,** 617–633
6. Shaham, O., Wei, R., Wang, T. J., Ricciardi, C., Lewis, G. D., Vasan, R. S., Carr, S. A., Thadhani, R., Gerszten, R. E., and Mootha, V. K. (2008) Metabolic profiling of the human response to a glucose challenge reveals distinct axes of insulin sensitivity. *Mol. Syst. Biol.* **4,** 214
7. Wopereis, S., Rubingh, C. M., van Erk, M. J., Verheij, E. R., van Vliet, T., Cnubben, N. H. P., Smilde, A. K., van der Greef, J., van Ommen, B., and Hendriks, H. F. J. (2009) Metabolic profiling of the response to an oral glucose tolerance test detects subtle metabolic changes. *PLoS ONE* **4,** e4525
8. Rubio-Aliaga, I., de Roos, B., Duthie, S., Crosley, L., Mayer, C., Horgan, G., Colquhoun, I., Le Gall, G., Huber, F., Kremer, W., Rychlik, M., Wopereis, S., van Ommen, B., Schmidt, G., Heim, C., Bouwman, F., Mariman, E., Mulholland, F., Johnson, I., Polley, A., Elliott, R., and Daniel, H. (2010) Metabolomics of prolonged fasting in humans reveals new catabolic markers. *Metabolomics* **7,** 375–387
9. Altmaier, E., Ramsay, S. L., Graber, A., Mewes, H.-W., Weinberger, K. M., and Suhre, K. (2008) Bioinformatics analysis of targeted metabolomics–uncovering old and new tales of diabetic mice under medication. *Endocrinology* **149,** 3478–3489
10. Illig, T., Gieger, C., Zhai, G., Römisch-Margl, W., Wang-Sattler, R., Prehn, C., Altmaier, E., Kastenmüller, G., Kato, B. S., Mewes, H.-W., Meitinger, T., Angelis, M. H. de, Kronenberg, F., Soranzo, N., Wichmann, H.-E., Spector, T. D., Adamski, J., and Suhre, K. (2010) A genome-wide perspective of genetic variation in human metabolism. *Nat. Genet.* **42,** 137–141
11. Roemisch-Margl, W., Prehn, C., Bogumil, R., Roehring, C., Suhre, K., and Adamski, J. (2012) Procedure for tissue sample preparation and metabolite extraction for high-throughput targeted metabolomics. *Metabolomics* **8,** 133–142
12. Weljie, A. M., Newton, J., Mercier, P., Carlson, E., and Slupsky, C. M. (2006) Targeted profiling: quantitative analysis of 1H NMR metabolomics data. *Anal. Chem.* **78,** 4430–4442
13. Lindinger, W., Hansel, A., and Jordan, A. (1998) On-line monitoring of volatile organic compounds at pptv levels by means of proton-transfer-reaction mass spectrometry (PTR-MS): medical applications, food control and environmental research. *Int. J. Mass Spectrom.* **173,** 191–241
14. Lucio, M., Fekete, A., Weigert, C., Wägele, B., Zhao, X., Chen, J., Fritsche, A., Häring, H.-U., Schleicher, E. D., Xu, G., Schmitt-Kopplin, P., and Lehmann, R. (2010) Insulin sensitivity is reflected by characteristic metabolic fingerprints–a Fourier transform mass spectrometric non-targeted metabolomics approach. *PLoS ONE* **5,** e13317
15. Suhre, K., and Schmitt-Kopplin, P. (2008) MassTRIX: mass translator into pathways. *Nucleic Acids Res.* **36,** W481–W484
16. Benjamini, Y., and Hochberg, Y. (1995) Controlling the false discovery rate: a practical and powerful approach to multiple testing. *J. Royal Stat. Soc. B (Methodological)* **57,** 289–300
17. Bartlett, K., and Eaton, S. (2004) Mitochondrial beta-oxidation. *Eur. J. Biochem.* **271,** 462–469
18. Eaton, S. (2002) Control of mitochondrial beta-oxidation flux. *Prog. Lipid Res.* **41,** 197–239

19. Ramsay, R. R. (2000) The carnitine acyltransferases: modulators of acyl-CoA-dependent reactions. *Biochem. Soc. Trans.* **28,** 182–186

20. Noland, R. C., Koves, T. R., Seiler, S. E., Lum, H., Lust, R. M., Ilkayeva, O., Stevens, R. D., Hegardt, F. G., and Muoio, D. M. (2009) Carnitine insufficiency caused by aging and overnutrition compromises mitochondrial performance and metabolic control. *J. Biol. Chem.* **284,** 22840–22852

21. Maher, A. D., Zirah, S. F. M., Holmes, E., and Nicholson, J. K. (2007) Experimental and analytical variation in human urine in 1H NMR spectroscopy-based metabolic phenotyping studies. *Anal. Chem.* **79,** 5204–5211

22. Begriche, K., Massart, J., Abbey-Toby, A., Igoudjil, A., Letteron, P., and Fromenty, B. (2008) β-Aminoisobutyric acid prevents diet-induced obesity in mice with partial leptin deficiency. *Obesity* **16,** 2053–2067

23. Rashed, M. S. (2001) Clinical applications of tandem mass spectrometry: ten years of diagnosis and screening for inherited metabolic diseases. *J. Chromatogr. B Biomed. Sci. Appl.* **758,** 27–48

24. Martins, A. M. (1999) Inborn errors of metabolism: a clinical overview. *Sao Paulo Med. J.* **117,** 251–265

25. Suhre, K., Shin, S.-Y., Petersen, A.-K., Mohney, R. P., Meredith, D., Wagele, B., Altmaier, E., Deloukas, P., Erdmann, J., Grundberg, E., Hammond, C. J., de Angelis, M. H., Kastenmuller, G., Kottgen, A., Kronenberg, F., Mangino, M., Meisinger, C., Meitinger, T., Mewes, H.-W., Milburn, M. V., Prehn, C., Raffler, J., Ried, J. S., Romisch-Margl, W., Samani, N. J., Small, K. S., Wichmann, H.-E., Zhai, G., Illig, T., Spector, T. D., Adamski, J., Soranzo, N., and Gieger, C. (2011) Human metabolic individuality in biomedical and pharmaceutical research. *Nature* **477,** 54–60

26. Zhao, X., Fritsche, J., Wang, J., Chen, J., Rittig, K., Schmitt-Kopplin, P., Fritsche, A., Häring, H.-U., Schleicher, E. D., Xu, G., and Lehmann, R. (2010) Metabonomic fingerprints of fasting plasma and spot urine reveal human pre-diabetic metabolic traits. *Metabolomics* **6,** 362–374

27. Gall, W. E., Beebe, K., Lawton, K. A., Adam, K.-P., Mitchell, M. W., Nakhle, P. J., Ryals, J. A., Milburn, M. V., Nannipieri, M., Camastra, S., Natali, A., and Ferrannini, E. (2010) alpha-Hydroxybutyrate is an early biomarker of insulin resistance and glucose intolerance in a nondiabetic population. *PLoS ONE* **5,** e10883.

28. Wang, T. J., Larson, M. G., Vasan, R. S., Cheng, S., Rhee, E. P., McCabe, E., Lewis, G. D., Fox, C. S., Jacques, P. F., Fernandez, C., O'Donnell, C. J., Carr, S. A., Mootha, V. K., Florez, J. C., Souza, A., Melander, O., Clish, C. B., and Gerszten, R. E. (2011) Metabolite profiles and the risk of developing diabetes. *Nat. Med.* **17,** 448–453